Performance of Dense Coding and Teleportation for Random States – Augmentation via Pre-processing

Rivu Gupta[1], Shashank Gupta[2], Shiladitya Mal[1], Aditi Sen (De)[1]

[1] *Harish-Chandra Research Institute and HBNI, Chhatnag Road, Jhunsi, Allahabad - 211019, India and*
[2] *S. N. Bose National Centre for Basic Sciences, Block JD, Sector III, Salt Lake, Kolkata - 700 106, India*

In order to understand the resourcefulness of a natural quantum system in quantum communication tasks, we study the dense coding capacity (DCC) and teleportation fidelity (TF) of Haar uniformly generated random multipartite states of various ranks. We prove that when a rank-2 two-qubit state, a Werner state, and a pure state possess the same amount of entanglement, the DCC of a rank-2 state belongs to the envelope made by pure and Werner states. In a similar way, we obtain an upper bound via the generalized Greenberger-Horne-Zeilinger state for rank-2 three-qubit states when the dense coding with two senders and a single receiver is performed and entanglement is measured in the senders:receiver bipartition. The normalized frequency distribution of DCC for randomly generated two-, three- and four-qubit density matrices with global as well as local decodings at the receiver's end are reported. The estimation of mean DCC for two-qubit states is found to be in good agreement with the numerical simulations. Universally, we observe that the performance of random states for dense coding as well as teleportation decreases with the increase of the rank of states which we have shown to be surmounted by the local pre-processing operations performed on the shared states before starting the protocols, irrespective of the rank of the states. The local pre-processing employed here is based on positive operator valued measurements along with classical communication and we show that unlike dense coding with two-qubit random states, senders' operations are always helpful to probabilistically enhance the capabilities of implementing dense coding as well as teleportation.

I. INTRODUCTION

The basic quantum information processing tasks like dense coding [1, 2] and teleportation [3] demonstrate the usefulness of quantum entanglement [4] in the field of quantum information science. In particular, the idea of dense coding (DC) is to employ prior quantum correlation between the sender and the receiver for enhancing classical message-carrying capacity while in teleportation, unknown state gets transferred to a remote location without physical transportation with the help of a shared entangled state and two bits of classical communication. Performance of dense coding which is dubbed as the dense coding capacity (DCC) of the shared channel is quantified by the number of messages in a unit of bits carried from the sender to the receiver [5–8]. On the other hand, in teleportation, the relevant figure of merit is the teleportation fidelity (TF) which measures the closeness between the state obtained by the receiver and the target state to be teleported at the sender's end [3, 9, 10]. Over the years, spectacular experiments have been performed to realize both the protocols by using photons, massive particles, nuclear magnetic resonance, etc. [11–15].

After their inception, these two protocols have been generalised in many ways. Going beyond bipartite scenario, dense coding has been extended to a scenario of multiple senders and multiple receivers, which enlarges the possibility of encoding-decoding strategies in various ways [2, 16–19]. In the case of multiple senders, it was shown that invoking more general encoding than unitary, collective encoding is better than the individual encoding [20] while for multiple receivers situated at far-apart locations, locally accessible information [21] plays a crucial role to obtain the DCC when receivers are allowed to perform local operations and classical communication (LOCC) for decoding [2, 19]. Similarly, original teleportation protocol which is commonly known as standard teleportation scheme (STS) also has been generalised which include telecloning [22], multi-port teleportation [23–25], teleportation with multiple sender-receiver pairs [26, 27], counterfactual teleportation [28], reusing teleportation channel [29].

In a realistic situation, ideal conditions to achieve perfect DCC and TF are never met due to noises in the channel and imperfections in the apparatuses. To circumvent this, Bennett *et al.* proposed a method of distillation [30–33] which is a collective pre-processing scheme involving many copies of shared noisy entangled states and LOCC for obtaining pure maximally entangled state, suitable for perfect DC and teleportation. The problem with distillation is that it requires a large number of resources and successfully works only when singlet fraction is above some threshold value [31]. In the context of teleportation, this problem has been resolved by invoking filtering operation which acts at the single copy-level and can probabilistically provide an output having high TF [33]. Surprisingly, it was also shown that for a certain class of states, a dissipative channel can activate teleportation power [34]. For two-qubit states, optimal teleportation protocol is known together with optimal filter [35]. Very recently, it has been shown that in higher dimension, filtering can also be effective for revealing hidden teleportation power of

shared Werner state [36] and a class of rank-deficient state used as channel [37]. In obtaining a quantum advantage in the dense coding protocol, coherent information [38] plays the role similar to singlet fraction in the case of teleportation and up to our knowledge, improving the DCC of a channel via filtering has not been investigated as yet.

On a different front, randomly generated density matrices [39–47] provide a vital tool for analyzing and studying the trends of typical states in state space. They not only arise naturally in the chaotic process [48] but also can be generated in a systematic manner based on randomness in the outcome of quantum measurement [46]. Moreover, against the intuition of observing random behavior, it has been found that random states show some universal properties – average quantum correlations among randomly generated states increase with the increase of the number of parties [33–36]. Random states were instrumental in disproving a long-standing conjecture in quantum information science regarding additivity of minimal output entropy [38] and in showing constructive feedback in presence of a non-Markovian noisy environment [49].

In the present work, we investigate the patterns of capabilities obtained from two prominent quantum communication tasks for Haar uniformly generated random shared channels. In particular, we estimate the distributions of the dense coding capacity of states having different ranks in three specific scenarios: (1) a single sender and a single receiver, (2) two senders and a single receiver, and (3) two senders and two receivers. Note that in the first two cases, the decoding is done by global operations while in the third situation, the encoded states can only be decoded via LOCC. We prove that the DCC of a rank-2 two-qubit state lies in the envelope of the DCC of a pure state and a Werner state when all of them possess the same amount of entanglement. We numerically confirm that such upper and lower bounds hold also for rank-3 and -4 two-qubit states. On the other hand, we show that when three-qubit generalized Greenberger-Horne-Zeilinger (gGHZ) [50] and a rank-2 state have the same amount of entanglement in the senders:receivers bipartition, the DCC of the gGHZ state is higher than that of the rank-2 three-qubit state. The mean of the frequency distribution for DCC is obtained numerically for random states which are shown to be in good agreement with analytical estimation. In all scenarios of DC and teleportation protocols, we observe that the efficiencies decrease with the increase of rank for the random states. We apply local pre-processing operations in the form of dichotomic positive operator valued measurements (POVM)s on the shared state before starting the protocol and report that the performance can be enhanced by such pre-processing mechanism for random states. Specifically, by employing three kinds of figures of merit, we establish that the local pre-processing at the sender's or the receiver's or both the ends can help to proba-bilistically improve the capacities, as well as the teleportation fidelities, especially in higher ranked random states. One should note here that the pre-processing operations exploited here cannot be included in the encoding-decoding strategies (cf. [20]).

The paper is organized in the following way. In Sec. II, we recapitulate the generation of random states of different ranks, the dense coding capacity, the teleportation fidelity, and the general dichotomic local POVM elements for pre-processing. In Sec. III, we provide our analytical results and numerical observations on dense coding capacity before pre-processing while the results obtained after local pre-processing is presented in Sec. IV. In Sec. V, observations and results on teleportation fidelity before and after pre-processing are reported. Finally, we conclude with a summary of results in Sec. VI.

II. DEFINITIONS: DENSE CODING CAPACITY AND TELEPORTATION CAPABILITY OF MULTIPARTITE RANDOM STATES

In this section, we briefly describe dense coding capacity involving an arbitrary number of senders and a single as well as two receivers and define the teleportation fidelity for two-qubit states. Since we perform DC and teleportation for randomly generated states, let us first elucidate the procedure for such simulations [40]. Haar uniform generation of pure states with arbitrary number of parties having complex coefficients, $x_i = a_i + ib_i$, (a_i and b_is are real numbers), where real numbers are taken from a Gaussian distribution with mean 0 and standard deviation unity, denoted by $G(0, 1)$ is performed. Random mixed states of various ranks can be obtained from an appropriate multipartite pure state after taking partial traces of suitable subsystem. For example, two-qubit density matrices with rank-2, -3, and -4 can be simulated from random tripartite pure states chosen in complex Hilbert spaces of $C^2 \otimes C^2 \otimes C^2$, in $C^2 \otimes C^2 \otimes C^3$ and $C^2 \otimes C^2 \otimes C^4$ respectively [40].

A. Dense Coding Capacity

Consider a multipartite communication channel formed by multiple senders, $S_1, S_2, \cdots, S_N$ and a single receiver, R in which classical information transmission via quantum states occurs. As originally proposed by Bennett and Weisner [1], it can be shown that if senders and a receiver apriori share an entangled state, $\rho^{S_1 S_2 \ldots S_N R}$, more bits of classical information can be encoded and sent to the receiver compared to a protocol with unentangled states. The maximum classical information accessible by the receiving party is called the dense coding capacity [5–8, 16]. We consider two scenarios depending on the number of senders and receivers as mentioned earlier.

1) N-senders and a single receiver (NS-1R). Suppose N-senders and a single receiver share an (N+1)-party quantum state, $\rho^{S_1 \cdots S_N R}$. The dense coding capacity in this case reads as

$$\mathbb{C}^{NS-1R}(\rho^{S_1 \cdots S_N R}) = \max[\log_2 d_{S_1} + \cdots + \log_2 d_{S_N},$$
$$\log_2 d_{S_1} + \cdots + \log_2 d_{S_N} + S(\rho^R) - S(\rho^{S_1 \cdots S_N R})] \tag{1}$$

where, $d_{S_1}, \cdots, d_{S_N}$ are the dimension of the senders' subsystems, $S_1, \cdots, S_N$, respectively. ρ_R is the reduced state at the receiver's end and $S(\sigma) = -\text{tr}(\sigma \log_2 \sigma)$ is the von-Neumann entropy. The first term represents the amount of classical information that can be sent only by using classical protocol while a quantum state is suitable for dense coding if $S(\rho^R) - S(\rho^{S_1 \cdots S_N R}) > 0$. Notice that for two-qubits involving a single sender and a single receiver (1S-1R), it reduces to $1 + S(\rho^R) - S(\rho^{SR})$.

2) N-senders and 2-receivers (NS-2R). Let us now consider that there are two receivers, R_1 and R_2, in the dense coding protocol which again involve arbitrary number of senders, $S_1, S_2, \cdots, S_N$, sharing an (N+2)-party quantum state, $\rho^{S_1 \cdots S_N R_1 R_2}$. In this situation, although we do not know the exact DCC, the upper bound is known [16]. Let 'k' senders, $S_1, \cdots, S_k$, send their parts of the shared state to the first receiver, R_1, while the remaining senders, $S_{k+1}, \cdots, S_N$, send their states to the second one, R_2. The upper bound on the dense coding capacity is then represented by

$$\mathbb{C}^{NS-2R}(\rho^{S_1 \cdots S_N R_1 R_2}) \leq \max[\log_2 d_{S_1} + \cdots + \log_2 d_{S_N},$$
$$\log_2(d_{S_1}) + \cdots + \log_2(d_{S_N}) + S(\rho^{R_1})$$
$$+ S(\rho^{R_2}) - \max(S(\rho^{S_1 \cdots S_k R_1}), S(\rho^{S_{k+1} \cdots S_N R_2}))] \equiv U^{NS-2R} \tag{2}$$

where $\rho^{R_1} = \text{tr}_{S_1 \cdots S_N R_2} \rho^{S_1 \cdots S_N R_1 R_2}$ and $\rho^{R_2} = \text{tr}_{S_1 \cdots S_N R_1} \rho^{S_1 \cdots S_N R_1 R_2}$ are the reduced states of the first and the second receiver respectively. Similarly, $\rho^{S_1 \cdots S_k R_1} = \text{tr}_{S_{k+1} \cdots S_N R_2} \rho^{S_1 \cdots S_N R_1 R_2}$ and $\rho^{S_{k+1} \cdots S_N R_2} = \text{tr}_{S_1 \cdots S_k R_2} \rho^{S_1 \cdots S_N R_1 R_2}$. We will investigate the behavior of the upper bound for the Haar uniformly generated four-qubit states where there are two senders and two receivers.

B. Teleportation Fidelity

In the teleportation protocol, the task is to send an unknown quantum state to the receiver. If a shared state is maximally entangled, such a task can be accomplished by performing the entangled measurements at the sender's side and communicating the outcomes to the receiver. Let us suppose that the sender, Alice and the receiver, Bob share an arbitrary bipartite state ρ^{SR}. The teleportation fidelity of ρ^{SR} can be expressed as [9, 10]

$$\mathbb{F} = \frac{d f + 1}{d + 1} \tag{3}$$

where $f = \max_{\{\phi\}} \langle \phi | \rho^{SR} | \phi \rangle$ with $\{\phi\}$ being the set of all maximally entangled two-qudit states and d is the dimension of the input state to be teleported. Notice that Alice and Bob have the freedom to apply any trace-preserving local quantum operations and classical communication (LQCC) in order to maximize f which is, in general, hard to perform even numerically.

Given a two-qubit state, ρ^{SR}, we can calculate the optimal teleportation fidelity by using the Horodecki's prescription [51], i.e.,

$$\mathbb{F}_{max} \leq \frac{1}{2}(1 + \frac{1}{3} \text{tr} \sqrt{C^\dagger C}) \tag{4}$$

where the elements of the matrix, $C = [C_{ij}]$, are given by $C_{ij} = \text{tr}[\rho^{SR}(\sigma_i \otimes \sigma_j)]$, where σ's are the Pauli spin matrices. Furthermore, if the state ρ^{SR} violates the Clauser-Horne-Shimony-Holt inequality [52, 53], i.e., if it satisfies $M(\rho^{SR}) > 1$ [51], where $M(\rho^{SR}) = (u_1 + u_2)$ with u_1 and u_2 being the highest two eigenvalues of the matrix $C^\dagger C$, the inequality (4) is replaced by an equality.

C. Preprocessing Operations

We know that the initial DCC or TF of a state can probabilistically be increased if some or all of the parties apply local pre-processing operations [20, 35, 54, 55]. If the DCC (TF) is initially in the classical region and after pre-processing, it gives a quantum advantage, we say that the state exhibits *hidden* DCC (TF). If the initial state already shows quantum advantage in dense coding (teleportation), and after preprocessing, the advantage gets improved with some positive probability, those states demonstrate *enhancements* in DCC (TF). For the present study, we apply the most general dichotomic POVMs [56–59] as local pre-processing operations.

• **General dichotomic POVMs:** The general dichotomic POVMs can be represented as

$$E_i^\pm = \lambda P_i^\pm + \frac{1 \pm \gamma_i - \lambda_i}{2} I \tag{5}$$

where λ_i is the sharpness parameter, such that $0 \leq \lambda_i \leq 1$, $|\lambda_i| + |\gamma_i| \leq 1$ and $E_i^+ + E_i^- = \mathbb{1}$, with $\mathbb{1}$ being the identity operator. $P_i^+ = \cos \frac{\theta_i}{2} |0\rangle + e^{i\phi_i} \sin \frac{\theta_i}{2} |1\rangle$ and its orthogonal projector is P_i^-. Here, i represents the party which applies the POVM. To find the optimal POVM, we have to maximize over the set of parameters, $\{\theta_i, \phi_i, \lambda_i\}$. If the shared state is two-qubits and both the parties perform local preprocessing before starting the protocol, we have to carry out maximization over six

parameters to evaluate maximal DCC (TF). In a mul-

tipartite shared state, $\rho^{S_1 \cdots S_N R}$, considering preprocessing operations performed by first k senders, the output state after the action of local POVMs is given by

$$\rho_P^{S_1 \cdots S_N R} = \frac{(\sqrt{E_{S_1}^{\pm}} \otimes \cdots \otimes \sqrt{E_{S_k}^{\pm}} \otimes \mathbb{1}_{S_{k+1}} \otimes \cdots \otimes \mathbb{1}_R) \rho^{S_1 \cdots S_N R} (\sqrt{E_{S_1}^{\pm\dagger}} \otimes \cdots \otimes \sqrt{E_{S_k}^{\pm\dagger}} \otimes \mathbb{1}_{S_{k+1}} \otimes \cdots \otimes \mathbb{1}_R)}{\mathrm{tr}[(\sqrt{E_{S_1}^{\pm}} \otimes \cdots \otimes \sqrt{E_{S_k}^{\pm}} \otimes \mathbb{1}_{S_{k+1}} \otimes \cdots \otimes \mathbb{1}_R) \rho^{S_1 \cdots S_N R} (\sqrt{E_{S_1}^{\pm\dagger}} \otimes \cdots \otimes \sqrt{E_{S_k}^{\pm\dagger}} \otimes \mathbb{1}_{S_{k+1}} \otimes \cdots \otimes \mathbb{1}_R)]}. \quad (6)$$

Notice that the DCC (TF) of the resulting state is investigated after maximizing over $3k$ parameters involved in k local POVMs.

III. DENSE CODING CAPACITY OF RANDOM STATES WITHOUT PREPROCESSING

Let us first present the behavior of dense coding capacity of Haar uniformly generated multipartite states. In particular, we analyze the frequency distributions in three scenarios.

Case 1. A single sender - a single receiver (1S-1R) pair shares two-qubit random states with different ranks.
Case 2. Two senders and a single receiver (2S-1R) have three-qubit Haar uniformly generated states having rank-1, -2, -3, -4, -5 and -6.
Case 3. Haar uniformly simulated four-qubit pure as well as states having rank -2, - 3 and -4 are initially distributed among two senders and two receivers (2S-2R) situated in distant locations.

Before proceeding further, note that quantum advantages are not obtained when the DCC, $\mathbb{C}$, is unity for 1S-1R, two for both 2S-1R and 2S-2R situations provided the dimension of each party is restricted to be two. In cases of 1S-1R and 2S-1R, if the shared state is pure, the second term in Eq. (1) vanishes and hence DCC reduces to the von Neumann entropy of the receiver's part. Since the entanglement of a pure bipartite state can uniquely be quantified by the von Neumann entropy of the local density matrix [30], the quantum advantage can always be achieved for all entangled pure states. For mixed two-qubit states, we will show below by proving a theorem that such a connection between shared entanglement and DCC cannot be established.

In a 2S-1R case, a relation between genuine multipartite entanglement content of the shared pure state and DCC does not hold [19] and to our knowledge, no such results are known for mixed three-qubit states which will also be established for rank-2 three-qubit states. In this work, we also concentrate on mixed three-qubit states with rank upto six.

Let us first investigate the behavior of dense coding capability of random states. Entire calculations and analysis are based on 5×10^4 Haar uniformly generated states for each case. In all these scenarios, the

normalized frequency distribution of DCC, given by $\mathcal{F}_{DC} = \frac{N_{DC}(C(\rho))}{N_S}$, with $N_{DC}(C(\rho))$ being the number of states having DCC $C(\rho)$ and N_S being the total number of simulated states, is calculated except in the situation of two senders and two receivers case where the normalized distribution of the upper bound is analysed, as depicted in Fig. 1. The observations in the figure are listed below:

1. Obtaining a quantum advantage in the DC protocol decreases with the increase of the rank of the states. It can be argued that such behavior is seen because the average entanglement content of the Haar uniformly generated states decreases with the rank of the states. However, such a simple explanation may not hold as we will show below.

2. Percentages of states showing DCC more than the classical bound are 50.09%, 4.80% and 0.30% for two-qubit states with rank-2, -3, and 4 respectively. For the 2S-1R DC scheme, it turns out to be 50.31%, 0.08% for rank-2 and rank-3 states while no states are found to give a quantum advantage from rank$\geq$4 random states. All pure states are good for classical information transmission.

3. The upper bound in the 2S-2R case showing quantum superiority is seen for 97.36% of rank-2 four-qubit states and for all pure random states. For higher ranks, unlike 2S-1R DC protocol, the above percentage decreases but remains significant, being 95.77% and 95.34% for ranks -3 and -4 respectively.

4. The pattern of $\mathcal{F}_{DC}$ also changes with rank as well as with the increase in the number of senders and receivers. Specifically, we observe that the fraction of states, showing nonclassical capacity decreases with the rank of the random states as shown in Fig. 1 (lower panel (right)), irrespective of the DC schemes. It can also be captured by computing the mean and standard deviation (SD) of the distribution which we will discuss in the succeeding sections. We will also study how the distribution changes with the introduction of preprocessing in terms of POVM by different figures of merits.
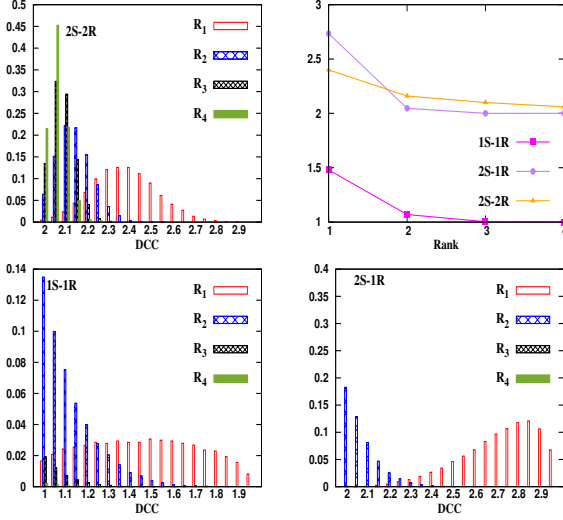
FIG. 1. (Color online) (Upper panel) and (Lower panel (left)). The normalized frequency distribution, $\mathcal{F}_{DC}$, of Haar uniformly generated states (vertical axis) against DCC (horizontal axis). Upper Panel. (Left) A single sender-single receiver (1S-1R) and (Right) single sender-two receivers (1S-2R) scenarios. Lower panel (left) two senders - two receivers (2S-2R). $R_1, \ldots R_4$ denotes the random states of rank-1 to rank-4. Lower Panel (right). Fraction of states having quantum advantage in dense coding vs. the rank of random states for three DC protocols. Notice that the large fraction of high rank mixed states have DCC in classical region and the general tendency to have quantum advantage decreases with the increase in rank. The rate of decrease of the upper bound for DCC with rank in 2S-2R case is significantly slower than the rate of DCC for 1S-1R and 2S-1R. All the axes are dimensionless.

To establish the fact that for mixed bipartite states, DC and entanglement content is not related, we will now show that the DCC of random states has a universal lower bound. In particular, we find that the DCC capacity of the Werner state, given by

$$\rho_W = p|\phi^+\rangle\langle\phi^+| + \frac{(1-p)}{4}I_4 \tag{7}$$

where $|\phi^+\rangle = \frac{1}{\sqrt{2}}(|00\rangle + |11\rangle)$ with $0 \leq p \leq 1$ and I_4 being the identity matrix in $C^2 \otimes C^2$, gives a lower bound for all randomly generated two-qubit states of rank-1 to rank-4 (see Fig. 2). Moreover, we observe that the DCC of Haar uniformly generated states with rank-2, -3 and -4 lies between the envelopes obtained for pure states, and the Werner states. Let us now prove the lower and upper bounds for rank-2 states.

Theorem 1. *The dense coding capacity of the arbitrary mixed two-qubit state of rank-2 in the 1S-1R case is upper bounded by the capacity of a pure state and lower bounded by a two-qubit Werner state when all of them possess the same amount of entanglement.*

Proof. Any two-qubit mixed state of rank-2 can be expressed as [60]

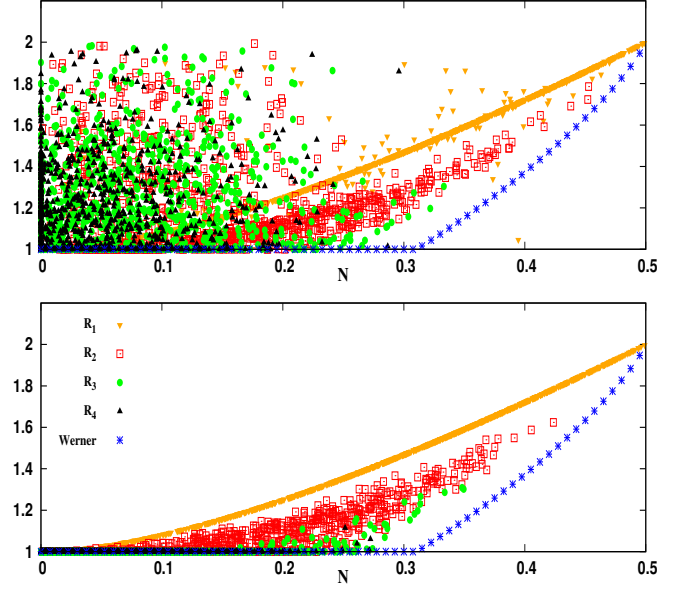$$\rho_2^2 = p_1|\psi_1\rangle\langle\psi_1| + (1-p_1)|\psi_2\rangle\langle\psi_2|, \tag{8}$$

FIG. 2. (Color online) Lower panel. Dense coding capacity of randomly generated two-qubit states (vertical axis) against entanglement (horizontal axis) which is quantified by negativity. Blue line represents the Werner state, ρ_W while the orange line represents the two-qubit pure state. Upper panel. The maximal cost of average DCC, defined later in Eq. (28) of random two-qubit states of different rank after two-sided POVMs is plotted with respect to negativity of the given initial state. We notice that the lower bound still holds after local POVMs applied by both the parties. The vertical axis is in bits while the horizontal axis is in ebits.

where $0 < p_1 < 1$, $|\psi_1\rangle = |0\eta_1\rangle + |1\eta_2\rangle$, $|\psi_2\rangle = |0\eta_1^\perp\rangle + |1\eta_2^\perp\rangle$, $|\eta_1\rangle = \cos\frac{\theta_1}{2}|0\rangle + \sin\frac{\theta_1}{2}|1\rangle$ and $|\eta_2\rangle = \cos\frac{\theta_2}{2}|0\rangle + \sin\frac{\theta_2}{2}|1\rangle$ with $|\eta_1^\perp\rangle$ and $|\eta_2^\perp\rangle$ being orthogonal states to $|\eta_1\rangle$ and $|\eta_2\rangle$ respectively, and $0 \leq \theta_i \leq \pi$, $i = 1, 2$. The entanglement here is quantified by the negativity [61–63] which is defined as the sum of the modulus of negative eigenvalues of the partially transposed state. In this case, negativity of ρ_2^2 in Eq. (8) reads as

$$\mathbb{N}_2^1 = \left|\frac{1}{4}\left[\sqrt{x} - 2(1-p_1)\right]\right| \tag{9}$$

$$\mathbb{N}_2^2 = \left|\frac{1}{4}\left[\sqrt{x} - 2p_1\right]\right|, \tag{10}$$

where $x = 2 + 4p_1(p_1 + 1) + 2(2p_1 - 1)\cos(\theta_1 - \theta_2)$. Note that for a fixed $p_1, \theta_i (i = 1, 2)$, $\mathbb{N}(\rho_2^2) = \max\{0, \mathbb{N}_2^1, \mathbb{N}_2^2\}$.

Let us first show the upper bound. The similar line of proof leads to the lower bound. An arbitrary two-qubit pure state written in a Schmidt decomposition reads as

$$|\psi\rangle = \cos\frac{\theta}{2}|0_S 0_R\rangle + \sin\frac{\theta}{2}|1_S 1_R\rangle \tag{11}$$

where $|0_{S(R)}\rangle$ and $|1_{S(R)}\rangle$ are the eigenvectors of the reduced density matrices corresponding to the sender (re-

ceiver) and the eigenvalues of the local density matrix are $\cos^2\frac{\theta}{2}$ and $\sin^2\frac{\theta}{2}$. The negativity of the pure state is the square root of the determinant of its reduced density matrix, i.e. $\sin\theta/2$. Equating entanglements of rank-2 and pure state, we obtain

$$\theta = \sin^{-1}(2\mathbb{N}). \tag{12}$$

On the other hand, the DCC of ρ_2^2 can be written as

$$\mathbb{C}(\rho_2^2) = 1 + H(\{\frac{1}{2}(1 - f_1(p_1)), \frac{1}{2}(1 + f_1(p_1))\})$$
$$- H(\{p_1, 1 - p_1\}), \tag{13}$$

where $H(\{p_i\}) = -\sum_i p_i \log_2(p_i)$ is the Shannon entropy of the probability distribution $\{p_i\}$, and $f_1(p_1) = \frac{1}{2}(1 - 2p_1)\cos(\frac{\theta_1 - \theta_2}{2})$ while $\mathbb{C}(|\psi\rangle) = 1 + H(\{\cos^2(\theta/2), \sin^2(\theta/2)\})$. Due to Eq. (12), $\mathbb{C}(|\psi\rangle)$ turns out to be a function of p_1, θ_1, and θ_2 which can help to prove the statement of the theorem, i.e., by showing inequality given by

$$H(\{\frac{1}{2}(1 - f_1(p_1)), \frac{1}{2}(1 + f_1(p_1))\}) - H(\{p_1, 1 - p_1\})$$
$$-H(\{\cos^2\frac{\theta}{2}, \sin^2\frac{\theta}{2}\}) < 0 \tag{14}$$

We substitute the value of θ in terms of p_1, θ_1, and θ_2 using Eq. (12), and numerically find that the inequality in (14) holds true for all values of the above parameters.

In a similar fashion, we find that the negativity of the Werner state, ρ_W, is $\frac{(1-3p)}{4}$. If entanglements of ρ_2^2 and ρ_W are equal, we get

$$p = \frac{1 - 4\mathbb{N}}{3}. \tag{15}$$

The DCC of ρ_W reads $1 + 1 + H(\{\frac{1+3p}{4}, \frac{1-p}{4}, \frac{1-p}{4}, \frac{1-p}{4}\})$, since the local entropy of the reduced system of the Werner state is unity. By using Eq. (15), we again numerically establish that DCC of any rank-2 state is always higher than that of the Werner state when both of them possess the same amount of entanglement for all values of p_1, θ_1 and θ_2.

Notice that although the proof is presented for real parameters, we observe that if $|\eta_i\rangle$, $i = 1, 2$ also have complex coefficients, the proof holds. $\square$

Remark 1. Numerically, we find that both the bounds remain true for all two-qubit states with rank-3 and -4.

Remark 2. Our numerical observations show that even after pre-processing, our theorem holds (see the upper panel in Fig. 2). It implies that when the receiver or both sender-receiver pair apply the local POVMs to activate the dense coding capability of shared states, the DCC of a random two-qubit state is still lower bounded by that of the Werner state having the same value of initial entanglement. However, the upper bound does not hold any more under local POVMs.
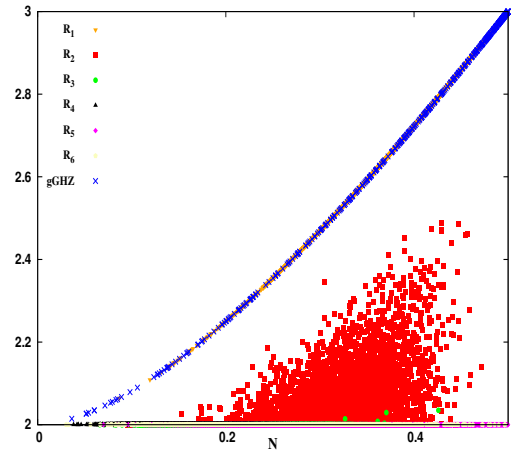

FIG. 3. (Color online) Dense coding capacity of Haar uniformly generated three-qubit states (vertical axis) vs. negativity (horizontal axis) in the bipartition of senders and the receiver. Blue line represents the generalized GHZ state, $|\phi_{gGHZ}\rangle$. Subscripts, i ($i = 1, \ldots 6$) of R_i denote the rank of the three-qubit states. The vertical axis is in bits while the horizontal axis is in ebits.

Theorem 2. *When negativities in the bipartition of senders and receivers of a three-qubit rank-2 state and the generalized GHZ state are equal, the dense coding capacity of the latter is always higher than that of the former.*

Proof. Any three-qubit rank-2 state, shared between $S_1 S_2 R$ can be written as [60]

$$\rho_3^2 = p_2 |\psi_3\rangle\langle\psi_3| + (1 - p_2)|\psi_4\rangle\langle\psi_4|, \tag{16}$$

where $0 < p_2 < 1$, and $|\psi_3\rangle = |0\eta_3\rangle + |1\eta_4\rangle$, $|\psi_4\rangle = |0\eta_3^\perp\rangle + |1\eta_4^\perp\rangle$, $|\eta_3\rangle = |0\eta_3'\rangle + |1\eta_4'\rangle$ and $|\eta_4\rangle = |0\eta_3''\rangle + |1\eta_4''\rangle$, with $|\eta_3'\rangle = \cos\frac{\theta_3}{2}|0\rangle + \sin\frac{\theta_3}{2}|1\rangle$, $|\eta_4'\rangle = \cos\frac{\theta_4}{2}|0\rangle + \sin\frac{\theta_4}{2}|1\rangle$, $|\eta_3''\rangle = \cos\frac{\theta_3'}{2}|0\rangle + \sin\frac{\theta_3'}{2}|1\rangle$, $|\eta_4''\rangle = \cos\frac{\theta_4'}{2}|0\rangle + \sin\frac{\theta_4'}{2}|1\rangle$ with $|\eta_3^\perp\rangle$ and $|\eta_4^\perp\rangle$ being orthogonal states to $|\eta_3\rangle$ and $|\eta_4\rangle$ respectively. Here $0 \le \theta_i$, $\theta_i' \le \pi$, $i = 3, 4$. The entanglement in terms of negativity [61] of rank-2 state in the $S_1 S_2 : R$ bipartition is

$$(\mathbb{N}_3^2)^1 = \frac{1}{8}\left[\sqrt{12 - 24p_2 + 16p_2^2 - (1 - 2p_2)y} - 4p_2\right],$$
$$\text{if } p_2 < 0.5 \tag{17}$$
$$(\mathbb{N}_3^2)^2 = \frac{1}{8}\left[\sqrt{4 - 8p_2 + 16p_2^2 + (1 - 2p_2)y} + 4p_2 - 4\right],$$
$$\text{if } p_2 > 0.5 \tag{18}$$

where $y = \cos(\theta_3 - \theta_3') + \cos(\theta_3 - \theta_4') + \cos(\theta_3' - \theta_4') + \cos(\theta_3 - \theta_4) + \cos(\theta_3' - \theta_4) + \cos(\theta_4' - \theta_4)$ and hence $\mathbb{N}(\rho_3^2) = \max\{0, (\mathbb{N}_3^2)^1, (\mathbb{N}_3^2)^2\}$ quantifies the negativity of ρ_3^2. For the three-qubit generalized GHZ (gGHZ) state,

$$|\phi_{gGHZ}\rangle = \cos(\theta_g/2)|0_{S_1}0_{S_2}0_R\rangle + e^{i\phi_g}\sin(\theta_g/2)|1_{S_1}1_{S_2}1_R\rangle \tag{19}$$

where $0 < \theta_g < \frac{\pi}{2}$ and $0 \leq \phi_g \leq \pi$, we have $\mathbb{N}(|\phi_{gGHZ}\rangle) = \frac{\sqrt{1-\cos 2\theta}}{2\sqrt{2}}$. When the entanglements of both the three-qubit rank-2 and the gGHZ states coincide, we find

$$\theta_g = \frac{\cos^{-1}(1 - 8\mathbb{N}_3^2)}{2} \tag{20}$$

On the other hand,

$$\mathbb{C}(\rho_3^2) = 2 + H(\{\frac{1}{2}(1 - f_2(p_2)), \frac{1}{2}(1 + f_2(p_2))\}) - H(\{p_2, 1 - p_2\}) \tag{21}$$

where $f_2(p_2) = \frac{1}{2\sqrt{2}}\sqrt{(1 - 2p_2)^2(2 + y)}$ while $\mathbb{C}(|\phi_{gGHZ}\rangle) = 2 + H(\{\cos^2(\theta_g/2), \sin^2(\theta_g/2)\})$. Mathematically, the statement of the theorem requires the following inequality to hold

$$H(\{\frac{1}{2}(1 - f_2(p_2)), \frac{1}{2}(1 + f_2(p_2))\}) - H(\{p_2, 1 - p_2\})$$
$$- H(\{\cos^2(\theta_g/2), \sin^2(\theta_g/2)\}) < 0. \tag{22}$$

We substitute the value of θ_g in terms of $p_2, \theta_3, \theta_4, \theta_3'$ and θ_4' using the relation, given in Eq. (20) and we numerically find that for all values of the above parameters, the inequality (22) holds true.

□

Remark 1. Like in two-qubit states, we also observe that the DCC of other mixed states of rank≥ 3 are also upper bounded by the DCC of the gGHZ state as shown in Fig. 3.

Remark 2. Our numerical results show that after preprocessing, some of the rank-2 states have higher DCC than that of the gGHZ state when both of them possess the same amount of initial entanglement. Hence, our theorem does not hold when the senders and the receiver apply local POVMs.

A. Analytical expression for mean DCC

Let us now derive the analytical expression of the mean dense coding capacity of Haar-uniformly generated two-qubit states of different ranks in the 1S-1R scenario. These analytical expressions match significantly well with our numerical results as obtained from numerical data in Fig. 1. From Eq. (1), the mean DCC for random two-qubit states can be rewritten as

$$\langle \mathbb{C}^{1S-1R}(\rho^{SR}) \rangle = 1 + \langle S(\rho^R) - S(\rho^{SR}) \rangle. \tag{23}$$

The mean entropy of a subsystem of dimension M, which is obtained through partial tracing from a pure state of dimension MK, can be expressed as [39]

$$\langle S_M \rangle \approx \log_2 M - \frac{M}{2K}. \tag{24}$$

TABLE I. Comparison between analytical (in Eq. (25)) and numerical values of $\langle \mathbb{C}^{SR} \rangle$.

Rank	Analytical			Numerical
	$N = 2$	$N = \dim/2$	$N = 100$	
2	0.481	0.735	1	1
3	0.15	0.489	0.667	0.711
4	0	0.366	0.5	0.536

For arbitrary two-qubit states, ρ^{SR}, $M = 4$. Depending upon the rank of the system, K can take value $1 \ldots 4$ for states with rank-$1, \ldots 4$ respectively. In order to calculate $\langle S(\rho^R) \rangle$ for the reduced state, we use the principle of purification of mixed states [64] according to which a mixed state is obtained from a higher dimensional pure state after tracing out appropriate subsystems of a pure state. If we assume that a $N + 2$- dimensional pure state leads to a single qubit state, the average entropy was found to be [65]

$$\langle S(\rho) \rangle = \frac{\log_2 e}{4^{N-1}} \frac{(2N-1)!}{(N-2)!(N-1)!}$$
$$\sum_{s=0}^{N-2} \binom{N-2}{s} \frac{(-1)^s}{(s+2)(2s+3)} \sum_{t=0}^{s+1} \frac{1}{2t+1} \tag{25}$$

Let us take $N = \frac{\text{dimension of initial pure state}}{2}$. The results for different ranks are enumerated below.

1. *Pure states.* In this case, $\langle S(\rho^{SR}) \rangle = 0$ and $\langle S(\rho^R) \rangle = 0.5$ which gives $\langle \mathbb{C}_1^{SR} \rangle = 1.5$ The subscript in $\mathbb{C}_1^{SR}$ denotes the rank of the state.

2. *Rank-2 states.* $\langle S(\rho^{SR}) \rangle = 1$ and $\langle S(\rho^R) \rangle$ is calculated using $N = 4$ in the formula (25) giving the value 0.735. Hence $\langle \mathbb{C}_2^{SR} \rangle = 0.735$.

3. *Rank-3 states.* By using Eqs. (24) and (25) with $N = 6$, we get $\langle S(\rho^{SR}) \rangle = \frac{4}{3}$ and $\langle S(\rho^R) \rangle = 0.822$ which leads to the mean DCC as $\langle \mathbb{C}_3^{SR} \rangle = 0.489$.

4. *Rank-4 states.* In this case, $\langle \mathbb{C}_4^{SR} \rangle = 0.366$ since $\langle S(\rho^{SR}) \rangle = \frac{3}{2}$ and $\langle S(\rho^R) \rangle = 0.866$ which is obtained by using $N = 8$.

Remark 1. The average of DCC obtained in the case of two-qubit states having rank-2, -3, -4 is below unity which implies that most of the states do not give quantum advantage in the dense coding protocol and hence average DCC decreases with the rank (cf. [49]).

Remark 2. Notice that the mean obtained by analysing the frequency distributions of DCC in Fig. 1 is much higher than the one reported above as also shown in Table I. We find that if we increase the dimension of the composite system, N, the analytical results match pretty well with the numerics. In fact with N = 100, the analytical and numerical results are in good agreement (see Table I).

IV. EFFECTS OF LOCAL PRE-PROCESSING ON THE DENSE CODING CAPACITY OF HAAR UNIFORMLY GENERATED STATES

The dense coding capacity, given in Eqs. (1) and (2), are obtained by optimizing over the unitary encoding performed by the sender(s) and the decoding by the receiver(s). However, it is expected that before starting the DC protocol, if one includes preprocessing on the shared states between the sender(s) and the receiver(s), the capacity can, in general, be enhanced with a certain probability. Since we deal with random states, and our aim is to find out the effects of preprocessing on random states, we illustrate by analyzing the situation where some of the senders and receivers or all of them apply the local dichotomic POVMs (in Eq. (5)) to activate the hidden DCC (to enhance DCC) when a particular choice of outcomes occur. To that end, we try to derive analytical conditions, which when satisfied, ensure that the state can exhibit enhanced DCC after pre-processing by POVMs. Let us define the following figures of merit to monitor the action of pre-processing operations on DCC.

Optimal increase in dense coding capacity (via POVM). After maximizing over all the parameters involved in local POVM, we concentrate on the DCC of the resulting state which is obtained when a specific measurement outcome clicks. The maximization is performed when POVM is performed by the sender(s) or the receiver(s) or both. We define the optimal increase in DCC due to the action of POVM by all the parties as

$$
\mathbb{O}_{DCC} = \max_{\{E_i^{o_i}\}} \mathbb{C} \left(\frac{(\otimes \sqrt{E_i^{o_i}})\rho(\otimes \sqrt{E_i^{o_i^\dagger}})}{\mathrm{tr}\left[(\otimes \sqrt{E_i^{o_i}})\rho(\otimes \sqrt{E_i^{o_i^\dagger}})\right]} \right), \quad (26)
$$

where the numerator denotes the output state, $\mathrm{tr}\left[(\otimes \sqrt{E_i^{o_i}})\rho(\otimes \sqrt{E_i^{o_i^\dagger}})\right]$ is the probability of obtaining the outcome to normalize the state, and $\{o_i\}$ represents the particular outcome that gives the maximal DCC. In case, some of the parties perform POVMs, we apply the identity operator on the rest as mentioned in Eq. (6). Although it may occur that several sets maximize the capacity, in a realistic situation, POVM is set to the optimal direction so that one of the possible choices of outcomes can occur. The enhancement can be measured by evaluating $\mathbb{O}_{DCC} - \mathbb{C}(\rho)$, with $\mathbb{C}(\rho)$ being the DCC of the original state before application of POVM.

Average cost of optimum dense coding capacity. Let us suppose that an outcome, o_i, of a particular POVM gives the maximal enhancement in the capacity of dense coding. The average cost of optimum dense coding capacity is then defined as

$$
\mathbb{A}^1_{DCC} = \sum_{\{o_i\}} p_{o_i} \mathbb{C}(\rho_{o_i}), \quad (27)
$$

where p_{o_i} is the probability of occurrence of a particular outcome of POVM, o_i and $\mathbb{C}(\rho_{o_i})$ represents the DCC of the normalized state after the action of POVM for that particular outcome, o_i. Note that the DCC for other outcome choices is calculated with the same choices of parameters in POVM which leads to the maximum increase in DCC calculated in Eq. (26).

Maximal cost of average dense coding capacity. After performing local POVMs by the sender(s) and the receiver(s), if we are interested to know the maximum enhancement that can occur in the dense coding protocol on average, we can evaluate the quantity, given by

$$
\mathbb{A}^2_{DCC} = \max_{\{\lambda_i, \theta_i, \phi_i\}} \left[\sum_{o_i} p_{o_i} \mathbb{C}(\rho_{o_i}) \right], \quad (28)
$$

where the maximization is performed over the set of parameters in POVM as given in Eq. (5), p_{o_i} is the probability of occurrence of a particular outcome and ρ_{o_i} is the normalized state after the action of pre-processing for that particular outcome. Notice that in the case of average cost of optimum dense coding capacity, we perform maximization to identify a single outcome that gives maximum DCC after POVM while in this case, maximization is performed to optimize the entire quantity which is written in the box parenthesis.

Based on the above three quantities, we now analyze the consequence of pre-processing acted by different combinations of the sender(s) and the receiver(s) mentioned before on the dense coding. Similar quantities will also be considered for teleportation where capacities will be replaced by fidelities.

1. Random two-qubit states after POVM: A single sender and a single receiver scenario

In this scenario, a sender, S, and a receiver, R, share a two-qubit random state, ρ^{SR} having different ranks. When the shared state is pure, we know that whenever the state is entangled, it is dense codable and hence the hidden DCC cannot be revealed after POVM although POVM can enhance the dense coding capability of the shared pure state. On the other hand, if the shared state is a two-qubit mixed state, we find that the mean DCC is below unity, as shown in Sec. III A, thereby implying that most of the Haar uniformly generated states do not show a quantum advantage in DC. For these states, either the sender or the receiver or both of them apply the pre-processing operations to extract the hidden DCC. We now present the exact conditions (in terms of eigenvalues of the shared state and reduced state before and after preprocessing) which have to be satisfied by the rank-2 mixed states for extracting the hidden DCC. It is important to mention here that when the pre-processing is completely positive trace preserving (CPTP) map which can be included in the encoding-

decoding process, it was shown that DCC can be enhanced by applying CPTP operations neither by the sender nor by the receiver [20].

Rank-2 state in 1S-1R scenario. Let the shared state, ρ^{SR}, be a rank-2 state. We denote its eigenvalues by x_1 and x_2, with $x_1 + x_2 = 1$ and $x_2 - x_1 = k_0$ while the reduced state at the receiver's side, $\rho^R = \mathrm{tr}_S(\rho^{SR})$, have eigenvalues x_1' and x_2' whose sum is still unity and difference is taken as $x_2' - x_1' = k_0'$. Obviously, since all the eigenvalues are positive, both $k_0, k_0' < 1$. The DCC (before pre-processing) expression can then easily be written in terms of the sum and difference of the eigenvalues of the density matrices as

$$\mathbb{C}(\rho^{SR}) = 1$$
$$-((1 - k_0') \log_2(1 - k_0') + (1 + k_0') \log_2(1 + k_0'))$$
$$+((1 - k_0) \log_2(1 - k_0) + (1 + k_0) \log_2(1 + k_0)). \quad (29)$$

After pre-processing has been applied, the resulting state is ρ_p^{SR} with eigenvalues summing to unity and having k as their difference. Similarly, for the reduced state after pre-processing (ρ_p^R), the sum of eigenvalues is unity, but their difference is k' and $0 \leq k, k' \leq 1$. In a similar spirit as above, we can write the dense coding capacity after pre-processing in terms of k and k' as

$$\mathbb{C}(\rho_p^{SR}) = 1 + S(\rho_p^R) - S(\rho_p^{SR}) = 1$$
$$-((1 - k') \log_2(1 - k') + (1 + k') \log_2(1 + k'))$$
$$+((1 - k) \log_2(1 - k) + (1 + k) \log_2(1 + k)). \quad (30)$$

It is straightforward to show that each entropy term, $S(\rho^R)$, $S(\rho_p^R)$, $S(\rho^{SR})$, and $S(\rho_p^{SR})$, in both $\mathbb{C}(\rho^{SR})$ and $\mathbb{C}(\rho_p^{SR})$, reaches their individual maximum values when k_0, k_0', k, k' are all vanishing. The DCC after pre-processing should possess two properties – the DCC after pre-processing is in the quantum region, i.e., $\mathbb{C}(\rho_p^{SR}) > 1$; and the DCC after pre-processing is greater than that of before, i.e., $\mathbb{C}(\rho_p^{SR}) > \mathbb{C}(\rho^{SR})$. We derive conditions for both these traits and argue whether both are necessary for a given rank or if we can work with either of them.

Condition for non-classical DCC after pre-processing. This condition demands that $S(\rho_p^R) - S(\rho_p^{SR}) > 0$. Since both these terms increase when their differences, i.e., k, k' approach to zero, and since after pre-processing we find numerically that the differences decrease i.e. $k < k_0$ and $k' < k_0'$, we propose the following:

Proposition 1. *The dense coding capacity after pre-processing is non-classical i.e. $S(\rho_p^R) - S(\rho_p^{SR}) > 0$, when k' is smaller than k, i.e. $k' < k$.*

The above condition follows from Eq. (30) and guarantees that $\mathbb{C}(\rho_p^{SR}) > 1$ although it does not ensure enhancement after pre-processing. States which satisfy it after pre-processing, will surely have non-classical DCC

and vice-versa. We see that this condition involves two eigenvalues and it may seem that it holds only for rank-2 states. However, our numerical analysis suggests that some rank-3 and -4 states after optimal POVMs are reduced to states with rank-2, and hence this condition is true for such two-qubit mixed states as well.

Condition for enhancing DCC after pre-processing. This condition demands that $S(\rho_p^R) - S(\rho_p^{SR}) > S(\rho^R) - S(\rho^{SR})$ which in turn depends on the changes occurred in the difference of eigenvalues before and after the pre-processing. In particular, we observe the following after POVM:

Proposition 2. *The dense coding capacity of rank-2 two-qubit states after pre-processing is greater than that of the state without pre-processing, if $(k_0' - k') > (k_0 - k)$.*

As noticed, when the difference between eigenvalues of the states vanishes, the individual entropies are maximized Therefore, we can get enhancement after pre-processing, if the rate in which k' in ρ_p^R goes closer to zero after changing from k_0' to k' is higher than k in ρ_p^{SR} which changes from k_0 to k, then the increase in $S(\rho_p^R)$ (from $S(\rho^R)$) is greater than the increase in $S(\rho_p^{SR}$ (from $S(\rho^{SR})$), thereby implying $\mathbb{C}(\rho_p^{SR}) > \mathbb{C}(\rho^{SR})$. We observe that among randomly generated two-qubit rank-2 states, 80.04% states to satisfy the above condition, although there are states, showing the advantage of pre-processing which do not satisfy the above criteria.
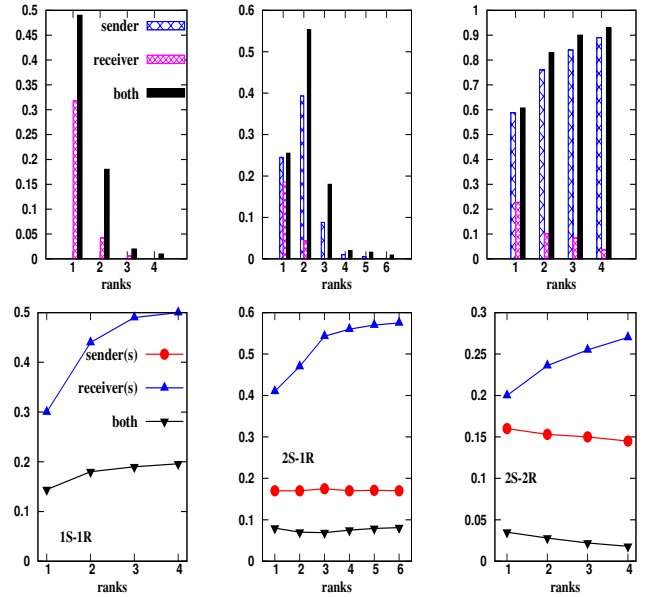

FIG. 4. (Color online) Upper Panel. Mean optimal increase in dense coding capacity, $\overline{O}_{DCC}$, (ordinate) in 1S-1R, 2S-1R and 2S-2R scenarios with varying rank of the shared state (abscissa). Lower Panel. Average probability of obtaining optimal increase in DCC, $\overline{p}_{O_{DCC}}$, in 1S-1R, 2S-1R, and 2S-2R DC protocol with ranks. All the axes are dimensionless.

TABLE II. Average optimal increase in DCC (Two-qubits). $\overline{O}_{DCC}$ denotes the optimal increase in DCC on average. "Both" and "Receiver" indicate that POVM is performed both by the sender, as well as the receiver, and the receiver only. "Before" represents the mean DCC for a given rank without local POVM.

	Before	Receiver	Both
		$\overline{O}_{DCC}$	$\overline{O}_{DCC}$
Rank-1	1.48	1.8	1.97
Rank-2	1.07	1.11	1.25
Rank-3	1.0043	1.01	1.034
Rank-4	1.00026	1.002	1.01

FIG. 5. (Color online) Upper Panel. The mean and standard deviation (shown as error bars) of average cost of optimum dense coding capacity, $\overline{A}^1_{DCC}$, for randomly generated states against the rank of the state in 1S-1R, 2S-1R. Lower Panel. Same quantity is plotted for two senders -two receivers. All the axes are dimensionless.

Let us now move to the scenario where two-qubit Haar uniformly generated states undergo pre-processing and we first address the issue of activation of hidden DCC, with the increase of ranks and with the number of parties doing POVM.

1. *Effects of rank.* As depicted in Fig. 1, the DCC of most of the mixed random states lies just above the classical limit if they have non-classical DCC and the percentage of states that have non-classical DCC decreases sharply with increasing rank.

First of all, we notice that if POVMs are performed by the sender, no increment in DCC is observed for two-qubit states (cf. [20]).

Secondly, after POVM, the *optimal increase in DCC* shows a rise on average (see Fig. 4), albeit with a finite probability. In Table II and Fig. 4, we illustrate $\overline{O}_{DCC} = \frac{\sum O_{DCC}(\rho^{SR})}{N_S}$ and $\overline{p}_{O_{DCC}} = \frac{\sum p_{O_{DCC}}(\rho^{SR})}{N_S}$, where N_S is the total number of states simulated and $p_{O_{DCC}}(\rho^{SR})$ is the probability of obtaining the outcome of the POVM which leads to the state having maximum increase in DCC. The increment and corresponding probability are complimentary to each other i.e. more increment occurs with lesser probability as it is visible from the upper and lower panels of Fig. 4. It is true that since most of the rank-4 and above randomly generated states without pre-processing are not advantageous for quantum DC, after pre-processing, the increase is also very low on average.

To analyse the average cost of optimum dense coding capacity and maximal cost of average DCC, we evaluate the mean and the standard deviation (SD) of these quantities for randomly generated two-qubit states. We observe that although POVMs by the receiver or both by the sender and the receiver do not help to increase the mean and the SD of these quantities for pure states, the pre-processing indeed enhances the capability of showing quantum advantages in the dense coding protocol in states with rank-2 and above as shown in the left columns of the upper panel in
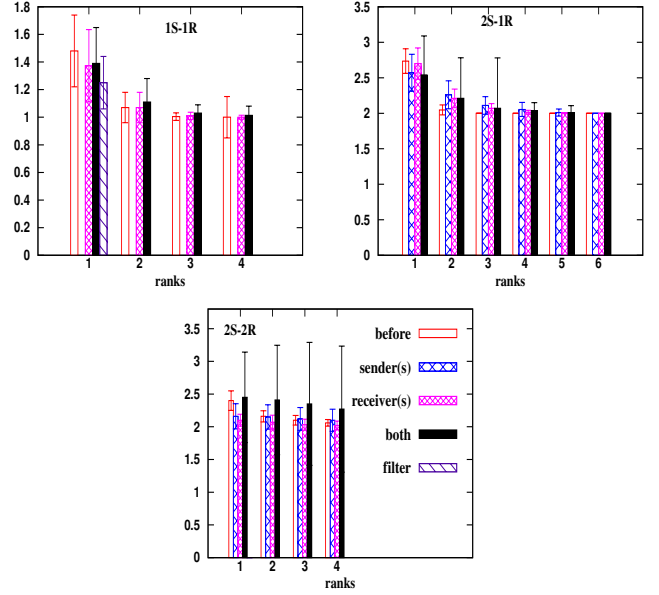
Figs. 5 and 6 as well as in Table III. When both the parties apply local POVMs, we observe that SD of $\mathbb{A}^1_{DCC}$ decreases with rank also although the SD obtained from the frequency distribution of DCC before pre-processing is lower than that of quantities after POVM.
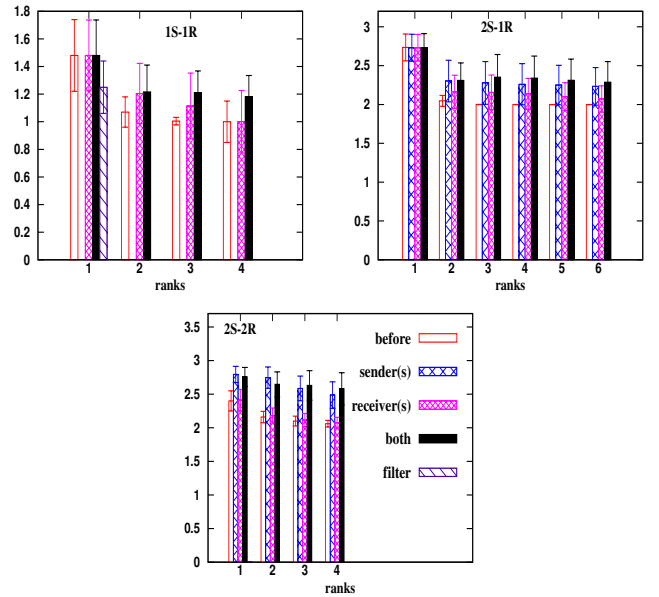

FIG. 6. (Color online) Upper Panel. The mean of maximal cost of average DCC, $\overline{A}^2_{DCC}$, against ranks. All the other specifications are same as in Fig. 5.

TABLE III. Mean of average cost of optimum dense coding capacity, $\overline{\mathbb{A}}^1_{DCC}$ and maximal cost of average dense coding capacity, $\overline{\mathbb{A}}^2_{DCC}$ for two-qubit random states. The label of the column, "Receiver" and "Both" indicate respectively the quantities after POVMs are applied by the receiver and after both the parties perform POVMs.

	Before	Receiver		Both	
		$\overline{\mathbb{A}}^1_{DCC}$	$\overline{\mathbb{A}}^2_{DCC}$	$\overline{\mathbb{A}}^1_{DCC}$	$\overline{\mathbb{A}}^2_{DCC}$
Rank-1	1.48	1.373	1.48	1.39	1.48
Rank-2	1.07	1.07	1.21	1.11	1.22
Rank-3	1.0043	1.01	1.15	1.03	1.21
Rank-4	1.00026	1	1.02	1.013	1.2

TABLE IV. Percentage of non-classical dense coding capacity for three-qubit states with rank-1 to rank-6 before and after POVMs. All the notations are the same as in Table III. Again "Before" denotes the percentage of states, giving a quantum advantage in the 2S-1R DC protocol without pre-processing.

	Before	Senders		Receiver		Both	
		$\mathbb{A}^1_{DCC}$	$\mathbb{A}^2_{DCC}$	$\mathbb{A}^1_{DCC}$	$\mathbb{A}^2_{DCC}$	$\mathbb{A}^1_{DCC}$	$\mathbb{A}^2_{DCC}$
Rank-1	100%	95.55%	99.96%	98%	99.99%	87.82%	99.83%
Rank-2	50.31%	86.72%	92.35%	92.28%	91.25%	45.83%	96.05%
Rank-3	0.08%	77.33%	79.64%	77.47%	78.45%	36.26%	87.36%
Rank-4	0%	58.1%	75.26%	38.91%	50.26%	30.6%	86.84%
Rank-5	0%	49.07%	73.96%	10.21%	48.85%	25.32%	85.28%
Rank-6	0%	39.78%	71.23%	7.26%	45.21%	18.96%	82.44%

2. *Effect of number of party doing pre-processing:* As mentioned before, in the two-qubit scenario, no POVMs by the sender enhances the DCC while the receiver's POVM help. However, when both parties apply POVMs, the enhancement is more pronounced than the case when only the receiver acts which can be confirmed by all the figures of merits considered here to measure the performance of DC in this case.

2. *Local POVMs by two senders are more effective than a single receiver*

Three-qubit Haar uniformly generated states with rank-1 to rank- 6 shared between two senders, S_1 and S_2 and a single receiver R are considered. All three-qubit pure random states show a quantum advantage in DC since the random states are typically genuinely multiparty entangled and hence $S(\rho^R)$ is positive for all of them. With the increase of rank, states showing non-classical DCC decreases and we do not find a single randomly generated state having rank≥4 which has $\mathbb{C}^{2S-1R}(\rho^{S_1 S_2 R}) > 2$ as shown in Table IV. Unlike two-qubit states, we observe that local POVMs applied by the senders can also help to enhance DCC probabilistically (see Fig. 4). Figs. 5 and 6 depict the enhancement on average by considering $\overline{\mathbb{A}}^1_{DCC}$ and $\overline{\mathbb{A}}^2_{DCC}$ due to the application of local POVMs before starting the protocol. In stark contrast with the two-qubit case, we observe that if senders can apply local POVMs, the maximal cost of average dense coding capacity gets

TABLE V. $\overline{\mathbb{A}}^i_{DCC}$, $i = 1, 2$ are listed for four-qubit states performing a DC protocol with two senders and two receivers.

	Before	Senders		Receivers		Both	
		$\mathbb{A}^1_{DCC}$	$\mathbb{A}^2_{DCC}$	$\mathbb{A}^1_{DCC}$	$\mathbb{A}^2_{DCC}$	$\mathbb{A}^1_{DCC}$	$\mathbb{A}^2_{DCC}$
Rank-1	2.4	2.16	2.757	2.1	2.412	2.45	2.792
Rank-2	2.16	2.15	2.646	2.07	2.182	2.41	2.747
Rank-3	2.1	2.12	2.586	2.032	2.115	2.35	2.63
Rank-4	2.06	2.1	2.487	2.021	2.074	2.27	2.58

more increased compared to the situation when only receiver performs POVM. Moreover, our results demonstrate that to obtain a quantum advantage in a multipartite DC scheme for random density matrices, pre-processing is essential.

3. *Effects of POVM on the upper bound of DCC with 2S-2R case*

Since two senders- two receivers DC scenario, only upper bound is known, we will now see whether upper bound can be enhanced by using pre-processing on the shared states. It is interesting to note here that there are states for which the upper bound on DCC by LOCC can be saturated. All the four-qubit pure states which are, in general, genuinely multipartite entangled states show $\mathbb{C}^{2S-2R}(\rho^{S_1 S_2 R_1 R_2}) \leq U^{2S-2R}(> 2)$. Interestingly, we observe that $\overline{\mathbb{A}}^i_{DCC}$, $i = 1, 2$ increases after applying optimal POVMs by both the parties even for pure states which is not true for DC protocol involving a single receiver. As seen from Figs. 4, 5 and 6 and Table V, for rank-2 to rank-4 four-qubit Haar uniformly generated states, the upper bound can again be improved substantially if the parties perform local POVM. Like DC with $2S - 1R$ scenario, senders can increase the upper bound more by acting POVMs compared to the case when receivers apply local POVMs which is prominent for $\overline{\mathbb{A}}^2_{DCC}$.

V. TELEPORTATION FIDELITY FOR RANDOM STATES

Let us now move to another quantum communication protocol, in particular, quantum teleportation. Let us first analyze the frequency distribution of the teleportation fidelity for random two-qubit states with different ranks in Fig. 7. It was realized from different studies that higher the entanglement, higher is the TF of the two-qubit states and all pure two-qubit states are good for quantum teleportation as well as they violate Bell inequality. It was found [10] that TF and violation of Bell inequality [52, 53] are connected. We observe that non classical TF for random states decreases with the increase of the ranks of the states. For example, we find that 48.2% rank-4 states have TF in the classical range while in rank-2 and rank-3, the percentages turn out to be 10.14% and 20.91% respectively.
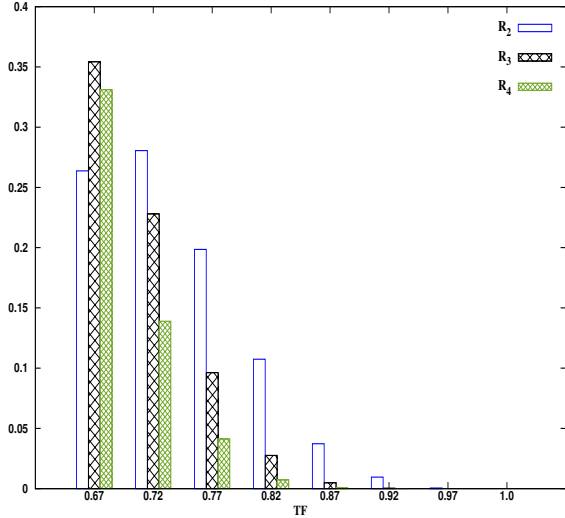
FIG. 7. (Color online) Normalized frequency distribution of TF, as defined in case of DC, for Haar uniformly generated two-qubit states (vertical axis) against non-classical TF (horizontal axis). All the axes are dimensionless.

Let us now show that with increasing rank, the relative number of states that possess local hidden variable model but gives non-classical fidelity increases. For example, 90% rank-2 states have $\mathbb{F} > 2/3$ out of which 67.9% are local while for rank-3 and -4, 93% and 98% are local among 73% and 51.8% states which show quantum advantage in teleportation respectively. Entire calculations and analysis are based on 10^6 Haar uniformly generated states for each case. We demonstrate the action of local pre-processing operations in revealing the hidden TF of such states. In this regard, we later present the exact POVM operations that either one party or both the party has to apply on the shared pure random state to achieve optimum TF.

A. Effect of local pre-processing on teleportation fidelity

Like the DC protocol, either the sender or the receiver or both the parties apply the local dichotomic POVMs (in Eq. (5)) to activate the teleportation fidelity with a non vanishing probability. We show that pre-processing sometimes allows us to enhance TF well beyond the classical limit (we call it as hidden TF) or to increase the TF beyond the initial fidelity which we refer it as enhanced TF. Note that if the post-processed state has TF below 2/3, we discard the state and follow the best classical protocol. As considered in the dense coding protocol, we define three quantities to monitor the action of pre-processing operations on TF. Specifically, we evaluate the optimal increase in TF, denoted by $\mathbb{O}_{TF}$, average cost of optimum TF, $\mathbb{A}^1_{TF}$ and maximal cost of average TF, $\mathbb{A}^2_{TF}$ which are respectively defined as in Eqs. (26), (27) and (28) by replacing $\mathbb{C}$ by $\mathbb{F}$.

TABLE VI. Mean of the average cost of optimum TF and maximal cost of average TF after applying POVMs. "Before" again represents TF of random states on average for a given rank, without the action of local POVM.

	Before	Sender		Receiver		Both	
		$\overline{\mathbb{A}}^1_{TF}$	$\overline{\mathbb{A}}^2_{TF}$	$\overline{\mathbb{A}}^1_{TF}$	$\overline{\mathbb{A}}^2_{TF}$	$\overline{\mathbb{A}}^1_{TF}$	$\overline{\mathbb{A}}^2_{TF}$
Rank 2	0.747	0.761	0.78	0.758	0.77	0.769	0.77
Rank 3	0.702	0.723	0.72	0.719	0.73	0.73	0.73
Rank 4	0.675	0.702	0.7	0.701	0.7	0.708	0.71

We now consider the action of pre-processing when the shared state is a random pure two-qubit state.
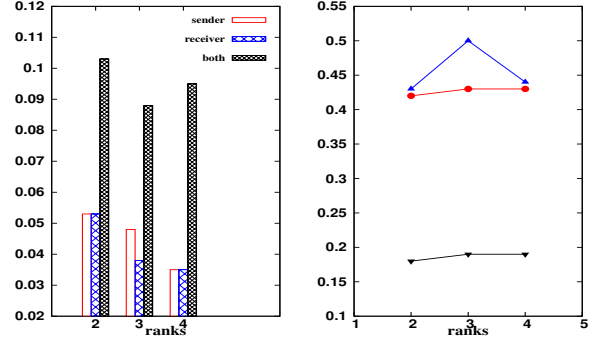

FIG. 8. (Color online) (Left) The optimum increment in teleportation fidelity on average, denoted by $\overline{\mathbb{O}}_{TF}$, vs. ranks of two-qubit states. (Right) $\overline{p}_{\mathbb{O}_{TF}}$ against ranks. Plots clearly show the trade off between the increment in TF and the success probability. All the axes are dimensionless.
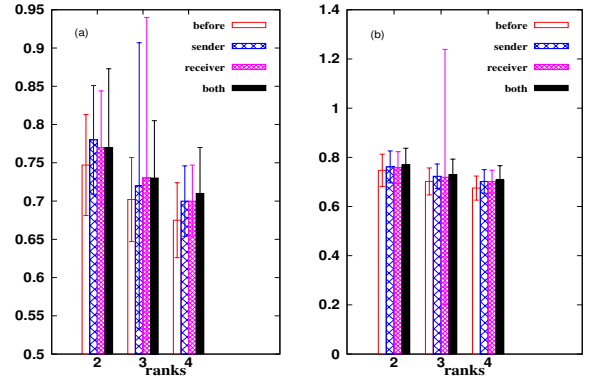

FIG. 9. (Color online) Left plot represents mean of average cost of optimum TF, $\overline{\mathbb{A}}^1_{TF}$ while right one is for $\overline{\mathbb{A}}^2_{TF}$ vs. ranks. SD are shown as error bars. All the axes are dimensionless.

• *TF after POVM on arbitrary two-qubit density matrices.* The effectiveness of local pre-processing operations in enhancing the TF of two-qubit random states is studied. In the two-qubit scenario, the optimal TF achievable from a shared two-qubit state is already known [34, 35]. Here, we compare the optimal fidelity already known with the POVMs considered in this paper.

TABLE VII. Percentage of states showing non classical teleportation fidelity before and after the actions of POVM. All other specifications are the same as in Table VI.

	Before	Sender		Receiver		Both	
		$\overline{\mathbb{A}}_{TF}^1$	$\overline{\mathbb{A}}_{TF}^2$	$\overline{\mathbb{A}}_{TF}^1$	$\overline{\mathbb{A}}_{TF}^2$	$\overline{\mathbb{A}}_{TF}^1$	$\overline{\mathbb{A}}_{TF}^2$
Rank 2	89.96%	95.99%	99.5%	94.88%	99.45%	87.68%	99.65%
Rank 3	79.09%	87.51%	99.26%	79.3%	99.17%	86.03%	99.58%
Rank 4	52.04%	82.62%	99%	78.87%	89.95%	83.51%	99.48%

1. *Efficacy of POVMs increases with ranks.* For a fixed rank, the number of states showing teleportation fidelity more than the classical bound increases probabilistically if the sender or the receiver or both perform local dichotomic POVMs (see Table VII). If one increases the rank, such increment is dramatic as quantified by $\overline{\mathcal{O}}_{TF}$, especially after the action of POVM by both the parties, as shown in Fig. 8. Unlike DC protocol with two-qubits, the sender can also help to increase the TF by applying local POVM.

2. We observe that the mean values of $\mathbb{A}_{TF}^i$, $i = 1, 2$ do not change so much after the action of POVMs which is different than the one observed in case of the DC protocol (comparing Table VI and Fig. 9 with Table III and Fig. 5).

3. In general, we observe that TF can be enhanced maximally when both the parties perform an optimal POVM although the probability of obtaining such outcome on average is less in this case compared to the one when the sender or the receiver performs POVM. On contrary, we find that for rank-2 random states, the average cost of optimum TF is more when pre-processing is on the sender's side only than on both sides. This is possibly due to the fact that during averaging, TF corresponding to some of the outcomes is very small and for both-sided POVMs, a number of such outcomes are more compared to the single-sided ones.

VI. CONCLUSION

It is hard to emphasize the role of dense coding and teleportation protocols to build a new arena of research dealing with quantum technologies. In laboratories, perfect dense coding capacity (DCC) and teleportation fidelity cannot be achieved due to the presence of different decohering factors and imperfections. Therefore, it is of utmost importance to devise a technique to restore quantum advantage as much as possible from low-performing states. It is usually done via pre-processing of channels which include distillation and filtering processes. By using these techniques, specific protocols are known for a specific class of states or for two-qubits.

In this work, we characterized TF for random two-qubit states and DCC for random two-, three- and four-qubits before any pre-processing. We then showed that substantial activation and enhancement in capacities, as well as fidelities, can happen after applying local pre-processing by the sender(s) and the receiver(s). For rank-2 two-qubit and three-qubit states, we analytically found that DCC of rank-2 states having the same amount of entanglement with pure two-qubit states and three-qubit generalized Greenberger-Horne-Zeilinger state is lower than that of the pure states, thereby establishing the fact that DCC and entanglement content of the shared states are not interconnected. We also proved that Werner state provides a lower bound on the DCC of rank-2 two-qubit states provided they possess the same amount of entanglement. Both upper and lower bounds obtained turned out to be true for any two- and three-qubit density matrices. Numerical simulations also showed that the lower bound holds for rank-2 states after local pre-processing. We defined three distinct figures of merit to access the advantage of local pre-processing. We found that the fraction of states exhibiting quantum advantage in DC and teleportation decreases with the increase of rank which can be overcome by means of local pre-processing operations before beginning the protocols. In the case of teleportation, it is interesting to see that for rank-3 and rank-4 states, 93% and 98% of states showing non-classical TF does not violate Clauser-Horne-Shimony-Holt Bell inequality [53].

APPENDIX: STATE DEPENDENT PRE-PROCESSING BY PURE STATES

In the case of pure two-qubit states, we know that all the states are dense codable as well as can give non classical teleportation fidelity. Any pure two-qubit state can be written in the Schmidt form [66] as

$$\rho^{SR} = \cos(\theta/2)|00\rangle + \sin(\theta/2)|11\rangle \tag{31}$$

where $|0\rangle$ and $|1\rangle$ are the orthonormal basis. Let us consider two situations, when the sender (the receiver) performs pre-processing and when both of them perform pre-processing.

1. *Pre-processing by sender (receiver)* Let us suppose the sender S (the receiver R) performs the following pre-processing operations on its part of the qubit [55].

$$P_S^+ = \begin{pmatrix} \tan(\theta) & 0 \\ 0 & 1 \end{pmatrix} ; P_S^- = \begin{pmatrix} \sqrt{1-\tan^2(\theta)} & 0 \\ 0 & 0. \end{pmatrix} \quad (32)$$

If S gets the outcome '+', the resultant state becomes a maximally entangled state whose dense coding capacity is 2 and the TF is unity. Note that following the notations in Eq. (6), $\sqrt{E_S^+} = P_S^+$ and the normalized state after the action of pre-processing is given by Eq.(6). The success probability is $\text{tr}[(P_S^+ \otimes \mathbb{1}_R).\rho^{SR}.(P_S^{+^\dagger} \otimes \mathbb{1}_R)]$.

2. *Both sender and receiver do pre-processing.* When both the sender and the receiver apply the following operations on their part of the qubit:

$$P_S^+ = \begin{pmatrix} \sqrt{\tan(\theta)} & 0 \\ 0 & 1 \end{pmatrix} ; P_S^- = \begin{pmatrix} \sqrt{1-\tan(\theta)} & 0 \\ 0 & 0 \end{pmatrix}$$
$$P_R^+ = \begin{pmatrix} \sqrt{\tan(\theta)} & 0 \\ 0 & 1 \end{pmatrix} ; P_R^- = \begin{pmatrix} \sqrt{1-\tan(\theta)} & 0 \\ 0 & 0. \end{pmatrix} (33)$$

and if they get the outcome '++', the output state is maximally entangled, giving maximal DCC and TF. As in Eq. (6), $\sqrt{E_S^+} = P_S^+$, $\sqrt{E_R^+} = P_R^+$ and the normalized state after the action of pre-processing is given by Eq.(6). The success probability is $\text{tr}[(P_S^+ \otimes P_R^+).\rho^{SR}.(P_S^{+^\dagger} \otimes P_R^{+^\dagger})]$. We find that the probability of success in both situations is equals to $2(\sin\theta)^2$. We find that although the above pre-processing leads to a higher $\mathbb{O}_{DCC}$ and $\mathbb{O}_{TF}$, compared to the state-independent method described in the paper, the average cost of optimum dense coding capacity, as well as the maximal cost of average DC (TF), turn out to be higher in the state-independent POVMs (see Figs. 5 and 6).

[1] C. H. Bennett and S. J. Wiesner, Phys. Rev. Lett. **69**, 2881 (1992).
[2] A. Sen(De) and U. Sen, Physics News **40**, 17 (2010).
[3] C. H. Bennett, G. Brassard, C. Crépeau, R. Jozsa, A. Peres, and W. K. Wootters, Phys. Rev. Lett. **70**, 1895 (1993).
[4] R. Horodecki, P. Horodecki, M. Horodecki, and K. Horodecki, Rev. Mod. Phys. **81**, 865 (2009).
[5] S. Bose, M. Plenio, and V. Vedral, J. Mod. Opt. **47**, 291 (2000).
[6] T. Hiroshima, J. Phys. A: Mathematical and General **34**, 6907 (2001).
[7] D. Bruß, G. M. D'Ariano, M. Lewenstein, C. Macchiavello, A. Sen(De), and U. Sen, Phys. Rev. Lett. **93**, 210501 (2014).
[8] M. Ziman and V. Bužek, Phys. Rev. A **67**, 042321 (2003).
[9] M. Horodecki, P. Horodecki, and R. Horodecki, Phys. Rev. A **60**, 1888 (1999).
[10] R. Horodecki, M. Horodecki, and P. Horodecki, Phys. Lett. A **222**, 21 (1996).
[11] S. Pirandola, J. Eisert, C. Weedbrook, A. Furusawa, and S. L. Braunstein, Nat. Phot. **9**, 641 (2015).
[12] T. Schaetz, M. D. Barrett, D. Leibfried, J. Chiaverini, J. Britton, W. M. Itano, J. D. Jost, C. Langer, and D. J. Wineland, Phys. Rev. Lett. **93**, 040505 (2004).
[13] K. Mattle, H. Weinfurter, P. G. Kwiat, and A. Zeilinger, Phys. Rev. Lett. **76**, 4656 (1996).
[14] D. Wei, X. Yang, J. Luo, X. Sun, X. Zeng, and M. Liu, Chinese Science Bulletin **49**, 423 (2004).
[15] J. Yin and *et. al.*, Science **356**, 1140 (2017).
[16] D. Bruß, M. Lewenstein, A. Sen(De), U. Sen, D. G. M., and C. Macchiavello, International Journal of Quantum Information **4**, 415 (2006).
[17] R. Prabhu, A. K. Pati, A. Sen (De), and U. Sen, Phys. Rev. A **87**, 052319 (2013).
[18] T. Das, R. Prabhu, A. Sen(De), and U. Sen, Phys. Rev. A **90**, 022319 (2014).
[19] T. Das, R. Prabhu, A. Sen(De), and U. Sen, Phys. Rev. A **92**, 052330 (2015).
[20] M. Horodecki and M. Piani, Journal of Physics A: Mathematical and Theoretical **45**, 105306 (2012).
[21] P. Badziag, M. Horodecki, A. Sen(De), and U. Sen, Phys. Rev. Lett. **91**, 117901 (2003).
[22] M. Murao, D. Jonathan, M. B. Plenio, and V. Vedral, Phys. Rev. A **59**, 156 (1999).
[23] S. Ishizaka and T. Hiroshima, Phys. Rev. Lett. **101**, 240501 (2008).
[24] S. Ishizaka and T. Hiroshima, Phys. Rev. A **79**, 042306 (2009).
[25] P. Kopszak, M. Mozrzymas, M. Studzinski, and M. Horodecki, arXiv:2008.00856 .
[26] A. Sen(De) and U. Sen, Phys. Rev. A **81**, 012308 (2010).
[27] S. Roy, T. Das, D. Das, A. Sen(De), and U. Sen, Ann. Phys. **422**, 168281 (2020).
[28] Q. Guo, L.-Y. Cheng, L. Chen, H.-F. Wang, and S. Zhang, Scientific Reports **5**, 8416 (2015).
[29] S. Roy, A. Bera, S. Mal, A. Sen (De), and U. Sen, arXiv:1905.04164.
[30] C. H. Bennett, G. Brassard, S. Popescu, B. Schumacher, J. A. Smolin, and W. K. Wootters, Phys. Rev. Lett. **76**, 722 (1996).
[31] D. Deutsch, A. Ekert, R. Jozsa, C. Macchiavello, S. Popescu, and A. Sanpera, Phys. Rev. Lett. **77**, 2818 (1996).
[32] C. H. Bennett, D. P. DiVincenzo, J. A. Smolin, and W. K. Wootters, Phys. Rev. A **54**, 3824 (1996).
[33] M. Horodecki, P. Horodecki, and R. Horodecki, Phys.

Rev. Lett. **78**, 574 (1997).

[34] P. Badziag, M. Horodecki, P. Horodecki, and R. Horodecki, Phys. Rev. A **62**, 012311 (2000).

[35] F. Verstraete and H. Verschelde, Phys. Rev. Lett. **90**, 097901 (2009).

[36] R. F. Werner, Phys. Rev. A **40**, 4277 (1989).

[37] J. Y. Li, X. X. Fang, T. Zhang, G. N. M. Tabia, H. Lu, and Y. C. Liang, arXiv:2008.01689 (2020).

[38] B. Schumacher and M. A. Nielsen, Phys. Rev. A **54**, 2629 (1996).

[39] V. M. Kendon, K. Życzkowski, and W. J. Munro, Phys. Rev. A **66**, 063210 (2002).

[40] I. Bengtsson and K. Życzkowski, *Geometry of Quantum States* (Cambridge University Press, 2017).

[41] P. Hayden, D. Leung, and A. Winter, Commun. Math. Phys **265**, 95 (2006).

[42] M. Enriquez, F. Delgado, and K. Życzkowski, Entropy **20**, 745 (2018).

[43] W. Kłobus, A. Burchardt, A. Kołodziejski, M. Pandit, T. Vértesi, K. Życzkowski, and W. Laskowski, Phys. Rev. A **100**, 032112 (2019).

[44] D. Gross, S. T. Flammia, and J. Eisert, Phys. Rev. Lett. **102**, 190501 (2009).

[45] S. Rethinasamy, S. Roy, T. Chanda, A. Sen(De), and U. Sen, Phys. Rev. A **99**, 042302 (2019).

[46] R. Banerjee, A. K. Pal, and A. Sen(De), Phys. Rev. A **101**, 042339 (2020).

[47] M. Hastings, Nature Physics **5**, 255 (2009).

[48] F. Haake, *Quantum Signatures of Chaos* (Springer-Verlag Berlin Heidelberg, 2010).

[49] R. Gupta, S. Gupta, S. Mal, and A. Sen (De), arXiv:2005.04009 (2020).

[50] M. Kafatos, *Bell's Theorem, Quantum Theory and Conceptions of the Universe, 69-72* (Springer-Verlag Berlin Heidelberg, 1989).

[51] R. Horodecki, P. Horodecki, and M. Horodecki, Phys. Lett. A **200**, 340 (1995).

[52] J. S. Bell, Physics **1**, 195 (1964).

[53] J. F. Clauser, M. A. Horne, A. Shimony, and R. A. Holt, Phys. Rev. Lett. **23**, 880 (1969).

[54] A. Peres, Phys. Rev. A **54**, 2685 (1996).

[55] N. Gisin, Physics Letters A **210**, 151 (1996).

[56] P. Busch, M. Grabowski, and P. J. Lahti, *Operational Quantum Physics* (Springer-Verlag Berlin Heidelberg, 1997).

[57] S. Yu, N.-l. Liu, L. Li, and C. H. Oh, Phys. Rev. A **81**, 062116 (2010).

[58] S. Mal, A. S. Majumdar, and D. Home, Mathematics **4**, 48 (2016).

[59] D. Das, S. Mal, and D. Home, Phys. Lett. A **382**, 1085 (2018).

[60] J. Walgate, A. J. Short, L. Hardy, and V. Vedral, Phys. Rev. Lett. **85**, 4972 (2000).

[61] G. Vidal and R. F. Werner, Phys. Rev. A **65**, 032314 (2002).

[62] K. Życzkowski, P. Horodecki, A. Sanpera, and M. Lewenstein, Phys. Rev. A **58**, 883 (1998).

[63] K. Życzkowski, Phys. Rev. A **60**, 3496 (1999).

[64] M. J. W. Hall, Phys. Lett. A **242**, 123 (1993).

[65] K. Życzkowski and H. J. . Sommers, J. Phys. A: Mathematical and General **34**, 7111 (2001).

[66] M. Nielsen and I. Chuang, *Quantum Computation and Quantum Information* (Cambridge University Press, 2000).